β-CaB$_4$O$_7$: A New Polymorph Synthesized under High-Pressure/High-Temperature Conditions

Hubert Huppertz

Department Chemie, Ludwig-Maximilians-Universität München, Butenandtstraße 5 – 13 (Haus D), D-81377 München, Germany

Reprint requests to Dr. H. Huppertz. E-mail: huh@cup.uni-muenchen.de

A new oxoborate β-CaB$_4$O$_7$ has been synthesized under high-pressure/high-temperature conditions from calcium oxide and boron oxide with a Walker-type multianvil apparatus at 7.7 GPa and 1100 °C. Single crystal X-ray structure determination of β-CaB$_4$O$_7$ revealed: $Pmn2_1$, $a = 1058.4(1)$, $b = 436.9(1)$, $c = 419.4(1)$ pm, $Z = 2$, $R1 = 0.0305$, $wR2 = 0.0587$ (all data). The compound is isotypic to the known oxoborates SrB$_4$O$_7$, PbB$_4$O$_7$, and EuB$_4$O$_7$ exhibiting a network structure of linked BO$_4$ tetrahedra. As a prominent feature of the tetrahedral network an oxygen atom is coordinated to three boron atoms. The relation of the crystal structure of the high-pressure phase β-CaB$_4$O$_7$ to the normal-pressure phase α-CaB$_4$O$_7$ as well as the relation to the isotypic phases MB$_4$O$_7$ (M = Sr, Pb, Eu) are discussed. The results of IR-spectroscopic investigations on β-CaB$_4$O$_7$ are also presented.

Key words: High-Pressure, Multianvil, β-CaB$_4$O$_7$, Borates, Crystal Structure

Introduction

Research on oxoborates provides distinctive opportunities for the discovery and identification of new compounds with interesting properties, *e.g.* materials for second harmonic generation or host materials for fluorescence [1 – 3].

From the structural point of view there is a great diversity grounded on the ability of boron to bind to three or four oxygen atoms, forming BO$_3$- or BO$_4$-groups which can be linked. Recently, we found that the use of high-pressure during the synthesis extends the compositional and structural scope. For example, in the system Ln$_2$O$_3$-B$_2$O$_3$ we were able to realize the new compositions Ln$_4$B$_6$O$_{15}$ (Ln = Dy, Ho) [4, 5] and α-Ln$_2$B$_4$O$_9$ (Ln = Eu, Gd, Tb, Dy) [6,7] under extreme high-pressure/high-temperature conditions. In contrast to all nearly 500 structurally characterized oxoborates, in which the linkage of BO$_3$- and BO$_4$-units occurs exclusively via corners, these new oxoborates are the first examples exhibiting edge-sharing BO$_4$ tetrahedra next to corner-sharing BO$_4$ tetrahedra.

Extending our investigations concerning oxoborates under high-pressure/high-temperature conditions, we performed syntheses in the system CaO-B$_2$O$_3$. This ternary system comprises several phases with the compositions Ca$_2$B$_2$O$_5$ (CaO : B$_2$O$_3$ = 2:1) [8 –

10], Ca$_2$B$_6$O$_{11}$ (2:3) [8,11], CaB$_2$O$_4$ (1:1) [12 – 19], Ca$_3$B$_2$O$_6$ (3:1) [20 – 23], and CaB$_4$O$_7$ (1:2) [24,25]. Investigations concerning the behaviour under high-pressure/high-temperature conditions were only performed on CaB$_2$O$_4$ [18]. As starting material for all high-pressure runs Marezio *et al.* used the orthorhombic normal pressure phase calcium metaborate CaB$_2$O$_4$-I [15,16], in which all boron atoms are triangularly coordinated. Increasing the pressure to a range of 1.2 – 1.5 GPa led to a second orthorhombic calciborite phase CaB$_2$O$_4$-II [14], exhibiting BO$_3$- and BO$_4$-groups in the same amount. The tetrahedrally coordinated part of boron atoms can be increased to 2/3 by a synthesis at 900 °C under a pressure of 1.5 – 2.5 GPa leading to CaB$_2$O$_4$-III [17]. Finally, in cubic CaB$_2$O$_4$-IV [18], synthesized in the range 2.5 – 4.0 GPa, all borons are tetrahedrally coordinated. The polymorphs of CaB$_2$O$_4$ are good examples for the Pressure-Coordination rule favouring the tetrahedral oxygen coordination of boron with increasing pressure.

In this paper we report about a new polymorph of CaB$_4$O$_7$. To distinguish between the two modifications we name the known normal-pressure phase "α-CaB$_4$O$_7$" [24,25] and the new high-pressure phase presented here "β-CaB$_4$O$_7$". The synthesis of β-CaB$_4$O$_7$ and its characterization *via* single crystal data are

Table 1. Crystal data and structure refinement for β-CaB$_4$O$_7$.

Empirical formula	β-CaB$_4$O$_7$
Molar mass	195.32 g/mol
Crystal system	orthorhombic
Space group	$Pmn2_1$ (No. 31)
Powder diffractometer	Stoe Stadi P
Radiation	Cu-K$_{\alpha 1}$ (λ = 154.06 pm)
Unit cell dimensions	a = 1059.00(4) pm
	b = 437.20(2) pm
	c = 419.49(2) pm
Volume	0.194(1) nm^3
Diffractometer	Enraf-Nonius Kappa CCD
Radiation	Mo-K$_\alpha$ (λ = 71.073 pm)
Unit cell dimensions	a = 1058.4(1) pm
	b = 436.9(1) pm
	c = 419.4(1) pm
Formula units per cell	Z = 2
Temperature	-73 °C
Calculated density	3.345 g/cm^3
Crystal size	$0.020 \times 0.025 \times 0.105$ mm^3
Detector distance	40.0 mm
Exposure time [°]	20 sec
Absorption coefficient	1.592 mm^{-1}
$F(000)$	192
θ Range	3.9° to 30.0°
Range in hkl	$\pm 14, \pm 6, \pm 5$
Scan type	φ/ω
Total no. reflections	3729
Independent reflections	594 (R_{int} = 0.0664)
Reflections with $I > 2\sigma(I)$	564 (R_σ = 0.0408)
Data/parameters	594 / 59
Absorption correction	numerical
Min./max. transmission ratio	0.70/0.91
Goodness-of-fit on F^2	1.098
Flack-Parameter	$-0.04(5)$
Final R indices [$I > 2\sigma(I)$]	$R1$ = 0.0277
	$wR2$ = 0.0576
R Indices (all data)	$R1$ = 0.0305
	$wR2$ = 0.0587
Extinction coefficient	0.009(6)
Largest diff. peak and hole	0.32 and -0.37 e/Å^3

described and a comparison with the normal-pressure modification α-CaB$_4$O$_7$ and the isotypic compounds SrB$_4$O$_7$ [27 – 29], PbB$_4$O$_7$ [27,30], and EuB$_4$O$_7$ [31] is made.

Experimental Section

According to eq. (1) the new polymorph β-CaB$_4$O$_7$ is synthesized from CaO (99%, Merck Darmstadt) and B$_2$O$_3$ (from H$_3$BO$_3$ (99.8%, Merck, Darmstadt) fired at 600 °C) in the molar ratio 1:2.

$$\text{CaO} + 2\,\text{B}_2\text{O}_3 \xrightarrow[1100\,°C]{7.7\,\text{GPa}} \beta - \text{CaB}_4\text{O}_7 \qquad (1)$$
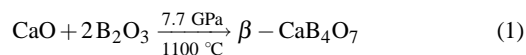
The components were mixed thoroughly in air and loaded into a 3.66 mm outside diameter, 0.33 mm wall thickness,

and 6.0 mm length hexagonal boron nitride cylinder which was sealed by a BN plate. The sample cylinder was placed in the center of a cylindrical resistance heater (graphite), with a variable (stepped) wall thickness in order to minimize the thermal gradient along the sample [32 – 35]. MgO rods filled the space at the top and at the bottom of the sample. A cylindrical zirconia sleeve surrounding the furnace provided thermal insulation. As a pressure medium Cr$_2$O$_3$-doped MgO octahedra (Ceramic Substrates & Components LTD., Isle of Wight) with an edge length of 18 mm were used. A hole was drilled into the octahedron, the cylindrical assembly positioned inside and contacted with a molybdenum ring at the top and a molybdenum plate at the bottom. The temperature was monitored using a Pt/Pt$_{87}$Rh$_{13}$ thermocouple inserted axially into the octahedral assembly with the hot junction in contact with the boron nitride cylinder. Eight tungsten carbide cubes separated by pyrophyllite gaskets (WidiaValenite, Essen, THM-F, edge length: 32 mm) with a truncation of 11 mm were used to compress the octahedron ("18/11 assembly" in conventional terminology) *via* a modified Walker-style split-cylinder multianvil apparatus [32]. For further details concerning the Walker-type module and multianvil experiments see [33 – 35].

For the synthesis of β-CaB$_4$O$_7$ the assembly was compressed over a period of 3 h to 7.7 GPa and heated to 1100 °C in the following 10 min. After holding this temperature for 10 min the sample was quenched by turning off the power with a quench rate of > 500 °C s^{-1}. After decompression the recovered octahedron was broken apart and the sample carefully separated from the surrounding BN. β-CaB$_4$O$_7$ was obtained as a single-phase, coarsely crystalline, colorless solid (yield: 30 mg per run).

Crystal Structure Analysis

The powder diffraction data of β-CaB$_4$O$_7$ were collected on a STOE Stadi P powder diffractometer with monochromized Cu-K$_{\alpha 1}$ radiation. The diffraction pattern was indexed with the program TREOR [36]. The lattice parameters (a = 1059.00(4), b = 437.20(2), c = 419.49(2) pm, Table 1) were obtained from least squares fits of the powder data. The correct indexing of the pattern was ensured by intensity calculations [37] taking the atomic positions from the structure refinements. The lattice parameters determined from the powder and the single crystal agreed well (Table 1).

Small single crystals were isolated by mechanical fragmentation and examined by Buerger precession photographs. Single crystal intensity data were collected from a regularly shaped colorless crystal (block) at -73 °C by use of an Enraf-Nonius Kappa CCD equipped with a rotating anode (Mo-K$_\alpha$ radi-

Table 2. Atomic coordinates and anisotropic displacement parameters ($\mathring{A}^2$) for β-CaB$_4$O$_7$ (space group $Pmn2_1$). U$_{eq}$ is defined as one third of the trace of the orthogonalized U$_{ij}$ tensor.

Atom	Wyckoff-position	x	y	z	U$_{eq}$
Ca1	2a	0	0.8003(2)	0.8968(2)	0.0086(2)
O1	4b	0.2252(2)	0.1375(4)	0.2453(4)	0.0052(3)
O2	4b	0.1366(2)	0.6488(3)	0.3323(3)	0.0056(3)
O3	4b	0.1336(2)	0.2773(3)	0.7497(4)	0.0050(3)
O4	2a	0	0.2151(5)	0.2982(5)	0.0049(5)
B1	4b	0.1206(2)	0.3264(5)	0.4107(9)	0.0047(4)
B2	4b	0.2504(2)	0.8215(5)	0.3856(9)	0.0047(4)

Atom	U$_{11}$	U$_{22}$	U$_{33}$	U$_{23}$	U$_{13}$	U$_{12}$
Ca1	0.0092(3)	0.0090(3)	0.0075(3)	0.0001(3)	0	0
O1	0.0059(7)	0.0059(7)	0.0039(7)	0.0003(6)	0.0005(6)	−0.0002(6)
O2	0.0046(6)	0.0040(7)	0.0082(10)	0.0007(5)	−0.0008(5)	−0.0002(5)
O3	0.0044(7)	0.0067(7)	0.0040(8)	0.0007(6)	0.0004(6)	0.0011(5)
O4	0.0048(10)	0.0041(9)	0.0057(11)	−0.0017(8)	0	0
B1	0.0055(9)	0.0041(9)	0.0046(10)	−0.0004(10)	0.0023(11)	0.0005(7)
B2	0.0056(9)	0.0043(9)	0.0041(9)	0.0012(11)	−0.0025(12)	−0.0017(7)

ation, λ = 71.073 pm). A numerical absorption correction was applied to the data. All relevant information concerning the data collection is listed in Table 1. According to the systematic extinctions $h0l$ with $h + l \neq 2n$, $h00$ with $h \neq 2n$, and $0k0$ with $k \neq 2n$ the space groups $Pmn2_1$ (no. 31) and $Pmnm$ (no. 59) were derived. The non-centrosymmetric group was found to be correct during the structure refinement. This was confirmed using the ADDSYM-routine of the program PLATON [38]. The starting positional parameters were deduced from an automatic interpretation of direct methods with SHELXS-97 [39] and the structure was successfully refined with anisotropic atomic displacement parameters for all atoms using SHELXL-97 (full-matrix least-squares on F^2) [40]. Final difference Fourier syntheses revealed no significant residual peaks (see Table 1). The positional parameters and interatomic distances of the refinements are listed in the Tables 2, 3, and 4. Listings of the observed/calculated structure factors and other details are available from the Fachinformationszentrum Karlsruhe, D-76344 Eggenstein-Leopoldshafen (Germany), email: crysdata@fiz-karlsruhe.de, by quoting the registry number CSD-412710.

Results and Discussion

The crystal structure of α-CaB$_4$O$_7$ (Fig. 1) is characterized by a boron-oxygen polyanion consisting of four crystallographically independent BO$_3$ triangles and four BO$_4$ tetrahedra linked *via* common vertices [25]. The eight triangles and tetrahedra form a [B$_8$O$_{14}$]$^{4-}$-unit, which is repeated throughout the

Table 3. Interatomic distances [pm] calculated with the single crystal lattice parameters in β-CaB$_4$O$_7$ (Standard deviations in parentheses; the letters a and b indicate symmetry equivalent oxygen atoms, which coordinate to the corresponding atoms at different interatomic distances).

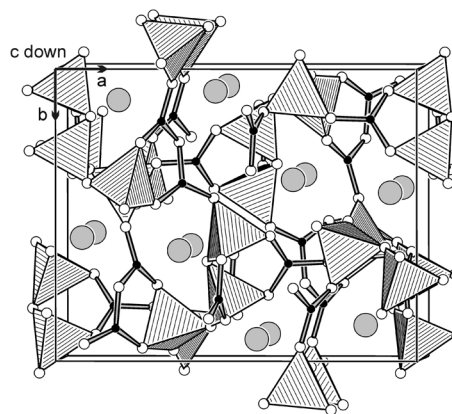|					
Ca1-O2a	242.1(2) 2×	B1-O3	144.4(4)	O1-B2a	152.4(3)
Ca1-O4a	247.4(2)	B1-O4	144.6(3)	O1-B2b	154.1(4)
Ca1-O3a	259.3(2) 2×	B1-O2	145.6(3)	O1-B1	154.5(3)
Ca1-O3b	275.7(2) 2×	B1-O1	154.5(3)	Ø = 153.7
Ca1-O2b	285.1(2) 2×		Ø = 147.3	
Ca1-O1a	298.9(2) 2×	B2-O3	142.1(3)	
Ca1-O4b	306.1(2)	B2-O2	143.9(3)	
Ca1-O4c	309.6(2)	B2-O1a	152.4(3)	
Ca1-O1b	316.1(2) 2×	B2-O1b	154.1(4)	
	Ø = 265.0		Ø = 148.1	

Fig. 1. Crystal structure of α-CaB$_4$O$_7$, view along [001]. The calcium cations are shown as large grey spheres, oxygen atoms as white spheres, and boron atoms as black spheres.

structure. The Ca atoms lie in seven- and eight-vertex polyhedra of oxygens atoms.

O3-B1-O4	110.8(2)	O3-B2-O2	120.1(2)	B2a-O1-B2b	117.0(2)
O3-B1-O2	110.8(2)	O3-B2-O1a	105.7(2)	B2b-O1-B1	115.8(2)
O4-B1-O2	110.7(2)	O2-B2-O1a	105.6(2)	B2b-O1-B1	119.8(2)
O3-B1-O1	107.1(2)	O3-B2-O1b	106.4(2)		Ø = 117.5
O4-B1-O1	107.9(2)	O2-B2-O1b	110.7(2)		
O2-B1-O1	109.4(2)	O1a-B2-O1b	107.6(2)		
	Ø = 109.5		Ø = 109.4		

Table 4. Interatomic angles [°] calculated with the single crystal lattice parameters in β-CaB$_4$O$_7$ (Standard deviations in parentheses; the letters a and b indicate symmetry equivalent atoms which coordinate to the corresponding atoms at different interatomic distances).

According to the synthetic conditions of high-pressure and high-temperature, β-CaB$_4$O$_7$ consists exclusively of corner-sharing BO$_4$ tetrahedra and is isotypic to the known phases SrB$_4$O$_7$ [27], PbB$_4$O$_7$ [27, 30], and EuB$_4$O$_7$ [31]. Table 5 shows the lattice parameters of the isotypic compounds. A comparison of the ionic radii for a given coordination number, *e. g.* C.N. = 10, reveals that Ca^{2+} (137 pm) has the lowest ionic radius in comparison to Sr^{2+} (150 pm), Eu^{2+} (149 pm), and Pb^{2+} (154 pm) [41], and consequently the lattice parameters of β-CaB$_4$O$_7$ have the lowest values. Fig. 2 gives a view of the crystal structure of β-CaB$_4$O$_7$ which exhibits a network of corner-sharing BO$_4$ tetrahedra forming channels along [00$\bar{1}$] built up from four- and six-membered rings. The calcium cations lie in the six-membered ring channels, while the four-membered ring channels remain empty. Fig. 3 gives a view along [100]. Of the four crystallographically independent oxygen atoms O1 (black spheres) shows an unusual feature in that it is bridging three BO$_4$ tetrahedra (O$^{[3]}$), while O2, O3, and O4 (white spheres) link two BO$_4$ tetrahedra (O$^{[2]}$). Three-coordinated oxygen atoms are rare in borate crystal chemistry. Next to SrB$_4$O$_7$ [27], PbB$_4$O$_7$ [27,30], and EuB$_4$O$_7$ [31] there exist only a few minerals like tunellite (SrB$_6$O$_9$(OH)$_2 \cdot$ 3 H$_2$O) [42], strontioginorite ((Sr,Ca)$_2$B$_{14}$O$_{20}$(OH)$_6 \cdot$ 5 H$_2$O) [43], aristarainite (Na$_2$Mg[B$_6$O$_8$(OH)$_4$]$_2 \cdot$ 4 H$_2$O) [44], and the high-pressure modification of B$_2$O$_3$ [45], which exhibit three-coordinate oxygen atoms. Recently, we reported on a new zinc borate with the composition β-ZnB$_4$O$_7$ which also exhibits oxygen in threefold coordination [46].

To examine topological connections between these oxoborates we calculated the cycle class sequence [47–50] for β-CaB$_4$O$_7$ showing the relative frequencies of B$_n$O$_n$-rings ($n = 3 - 10$), which is identical to the cycle-class sequences of MB$_4$O$_7$ (M = Sr, Pb, Eu). Table 6 shows the calculated ring sizes compared to β-ZnB$_4$O$_7$ and to the corresponding α-modifications. Interestingly, the phases MB$_4$O$_7$ (M = Ca, Sr, Pb, Eu) exhibit identical ring sizes up to a B$_n$O$_n$-ring size of

Table 5. Cell dimensions of the isotypic tetraborates MB$_4$O$_7$ (M = Ca, Sr, Eu, Pb) in the orthorhombic space group $Pmn2_1$.

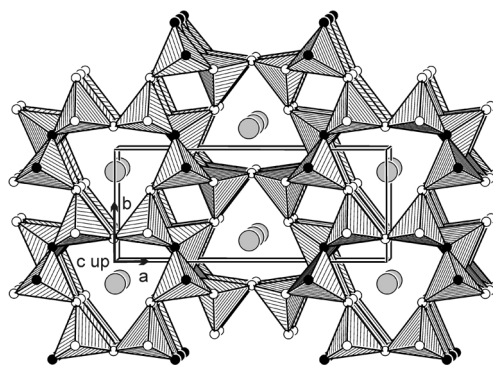|		a[pm]	b[pm]	c[pm]
β-CaB$_4$O$_7$	[this work]	1059.00(4)	437.20(2)	419.49(2)
SrB$_4$O$_7$	[28]	1070.6(10)	443.1(4)	423.7(4)
SrB$_4$O$_7$	[29]	1072.4(2)	444.7(3)	423.92(11)
EuB$_4$O$_7$	[31]	1073.1(1)	443.5(1)	424.0(1)
PbB$_4$O$_7$	[28]	1084.0(10)	445.7(4)	424.4(4)
PbB$_4$O$_7$	[30]	1086.0(3)	446.3(3)	425.1(2)

Fig. 2. Crystal structure of β-CaB$_4$O$_7$, view along [00$\bar{1}$]. The calcium cations are shown as large grey spheres, O$^{[2]}$ coordinated oxygen atoms as white spheres, and O$^{[3]}$ coordinated oxygen atoms as black spheres.

$n = 10$ as β-ZnB$_4$O$_7$ with differences in their frequency of occurrence for n larger than six.

An examination of the B-O distances in β-CaB$_4$O$_7$ (Table 3) shows variations between 142 and 155 pm. The average value is 148 pm which corresponds to the average B-O distance of 147 pm [51] in tetrahedral BO$_4$-units of most oxoborates. As expected, the bonds to three-coordinated oxygen atoms O$^{[3]}$ are significantly longer (152 – 155 pm) than the average with compensation by shortening of other bonds. Longer bonds can also be found in the oxoborates SrB$_4$O$_7$ [28,29], PbB$_4$O$_7$ [30], EuB$_4$O$_7$ [31], and β-ZnB$_4$O$_7$ [46], where the average B-O distances of 155.0, 155.4, 154.4, and 155.3 pm in the OB$_3$-groups correspond to the average distance of 153.7 pm found in this work. The O-B-O angles in the two crystallographi-

Table 6. Cycle class sequences [47 – 50] of α-CaB$_4$O$_7$ and β-CaB$_4$O$_7$ in comparison to the tetraborates of Zn, Sr, Pb, and Eu.

Ring size n	3	4	5	6	7	8	9	10
α-CaB$_4$O$_7$	12	4	0	0	0	4	16	40
β-CaB$_4$O$_7$	4	4	8	20	44	124	336	928
MB$_4$O$_7$ (M = Sr, Pb, Eu)	4	4	8	20	44	124	336	928
α-ZnB$_4$O$_7$	16	8	0	0	0	0	0	0
β-ZnB$_4$O$_7$	4	4	8	20	40	128	312	958
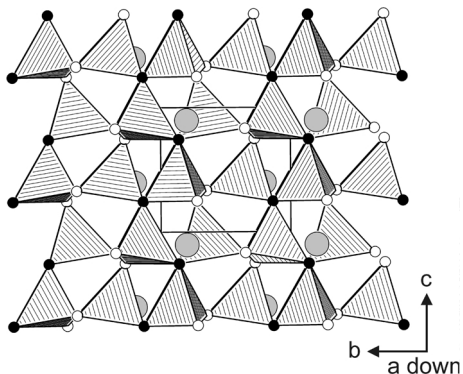
Fig. 3. Crystal structure of β-CaB$_4$O$_7$, view along [100]. The calcium cations are shown as large grey spheres, O$^{[2]}$ coordinated oxygen atoms as white spheres, and O$^{[3]}$ coordinated oxygen atoms as black spheres.

cally independent BO$_4$-tetrahedra are between 106° and 120° (Table 4) with an average value of 109.4°. The O-B-O angles in the OB$_3$-group are 117.0(2)°, 115.8(2)°, and 119.8(2)° with a mean value of 117.5° (Table 4).

In contrast to α-CaB$_4$O$_7$, where the Ca^{2+}-ions are coordinated by seven (228 – 258 pm) or eight (234 – 289 pm) oxygen atoms, the coordination number is drastically increased to 15 in the high-pressure polymorph β-CaB$_4$O$_7$. The Ca-O distances vary between 242 and 316 pm with an average value of 265 pm (Table 3). Although not all oxygen atoms are nearest neighbours, the high coordination number is confirmed by MAPLE-calculations. The next oxygen atom in the coordination sphere of the Ca^{2+}-ions appears at a distance of 358 pm indicating a clear break between coordinating and non-coordinating oxygen atoms. The isotypic borate SrB$_4$O$_7$ exhibits nine oxygen atoms in the next and additional six atoms in the next-nearest coordination sphere (263 – 320 pm) [28].

A similar increase of the coordination number can be observed in the high-pressure polymorphs of CaB$_2$O$_4$. The modifications CaB$_2$O$_4$-I [15,16] and CaB$_2$O$_4$-II [14] have Ca^{2+} in eightfold-coordination,
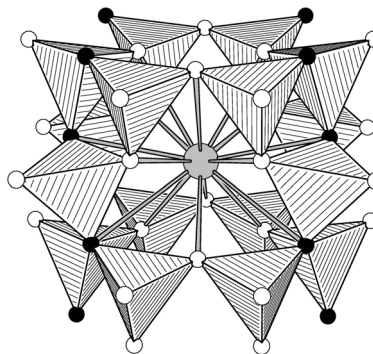
Fig. 4. Coordination of Ca^{2+} (grey sphere) in the crystal structure of β-CaB$_4$O$_7$.

but in CaB$_2$O$_4$-III [17] the coordination of one Ca^{2+} is increased to 10 (230 – 307 pm), and finally in CaB$_2$O$_4$-IV [18] all Ca^{2+} are coordinated by 12 oxygen atoms (239 – 314 pm).

β-CaB$_4$O$_7$ can be classified with the help of the "**F**undamental **B**uilding **B**lock"-conception (FBB) of Burns et al. [52, 53]. Fig. 5 is a view of the crystal structure of β-CaB$_4$O$_7$ along [0$\bar{1}$0], with the part of BO$_4$ tetrahedra which represent the fundamental building block encircled. This unit is built up by a three-membered ring of tetrahedra <3☐>, with one of the threefold coordinated oxygen atoms (O$^{[3]}$, black spheres) in the ring decorated with another tetrahedron (☐). As the O$^{[3]}$ element is the outstanding structural feature of this structure, the descriptor for this part is written as [O]<3☐>|☐| indicating O$^{[3]}$ as the central atom ([O]) decorated with a three-membered ring <3☐> and a single tetrahedron ☐. As this part occurs twice in the fundamental building block the complete notation is 8☐:{[O]<3☐>|☐|}{[O]<3☐>|☐|}. This unique FBB is repeated only by translation to give the complete network structure of BO$_4$ tetrahedra. The FBB presentation is much simpler, if rotational elements can also be used to build up the network. In this case the FBB notation is 4☐:[O]<3☐>|☐|, which corresponds to half of the previous form. There are several examples in the literature (e.g.: fabianite: 2Δ4☐:<Δ2☐>=<4☐>=<Δ2☐> [54] or brianroulstonite: 6Δ6☐:<Δ☐Δ☐Δ☐Δ☐Δ☐Δ☐> [55]), where the authors [53] preferred a graphically clearer fundamental building block using the smallest unit on cost of a unique cluster which would need only translation elements. We prefer the unique FBB 8☐:[O]{<3☐>|☐|}{[O]<3☐>|☐|}, for which only transitional elements are necessary.
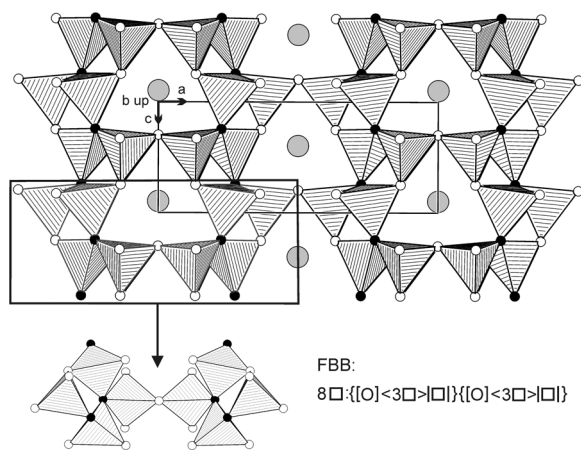
Fig. 5. The fundamental building block in the crystal structure of β-CaB$_4$O$_7$, view along [0$\bar{1}$0].

MAPLE-values (**Ma**delung **P**art of **L**attice **E**nergy) [56–58] were also calculated for β-CaB$_4$O$_7$ to compare the data with the normal-pressure modification α-CaB$_4$O$_7$ [24,25] and the MAPLE-values received for the binary components CaO and high-pressure B$_2$O$_3$-II [45]. For β-CaB$_4$O$_7$ we obtained a value of 47876 kJ/mol in comparison to 47665 kJ/mol calculated for α-CaB$_4$O$_7$ (deviation: 0.4%), and a value of 47924 kJ/mol (deviation: 0.1%) starting from the binary oxides [1 × CaO (4048 kJ/mol) + 2 × B$_2$O$_3$-II (21938 kJ/mol)].

Also bond-valence sums were calculated for all atoms using the bond-length/bond-strength concept (ΣV) [59,60] and the CHARDI concept (**Char**ge **Di**stribution in Solids) (ΣQ) [61]. As bond-valence parameters for the bond-length/bond-strength concept we used $R_{ij} = 137.1$ for B-O bonds and $R_{ij} = 196.7$ for Ca-O bonds [60]. Table 7 gives a comparison of the charge distribution calculated with both concepts. The values confirm supposed formal ionic charges of Ca^{2+}, B^{3+}, and O^{2-}.

The high-pressure structure of β-CaB$_4$O$_7$ is a representative example for the validation of the Pressure-Homologue Rule [26]. Like the chlorides of sodium, potassium, and rubidium (C.N. = 6) which transform under high-pressure to the structure type of their highest homologue caesium chloride (C.N. = 8), α-CaB$_4$O$_7$ also transforms to the structure of its higher homologue SrB$_4$O$_7$ [28,29]. The highest homologue in this series of tetraborates is monoclinic BaB$_4$O$_7$ [62]. As BaB$_4$O$_7$ exhibits BO$_3$- next to BO$_4$-units, it is improbable to represent a structure type

Table 7. Charge distribution in β-CaB$_4$O$_7$ calculated with the bond-length/bond-strength conception (ΣV) [59, 60] and the CHARDI conception (ΣQ) [61].

	Ca	B1	B2	O1	O2	O3	O4
ΣV	+1.93	+3.06	+3.02	−1.92	−2.01	−2.02	−1.89
ΣQ	+1.94	+2.98	+3.05	−1.77	−2.09	−2.13	−2.01

which would fulfil the requirements of a high-pressure phase.

SrB$_4$O$_7$ (SBO) was shown to be a potential NLO material with excellent mechanical and optical properties including a high powder SHG coefficient, high optical damage threshold, and high hardness, *etc.* [63]. We have started to investigate related properties of β-CaB$_4$O$_7$. Temperature dependent *in situ* powder diffraction studies have already shown that β-CaB$_4$O$_7$ is stable up to a temperature of 800 °C.

Infrared absorption spectroscopy

The infrared (IR) spectrum of β-CaB$_4$O$_7$ (Fig. 6) was recorded on a Bruker IFS 66v/S spectrometer with a scanning-range from 400 to 4000 cm^{-1}. The sample was thoroughly mixed with dried KBr (5 mg sample, 500 mg KBr) in a glove box under dried argon atmosphere.

Fig. 6 shows the section 2200 to 400 cm^{-1} of the IR spectrum of β-CaB$_4$O$_7$. The spectrum of the isotypic phase SrB$_4$O$_7$ reported by Weir *et al.* [64] shows very similar bands (Table 8). Additional absorptions observed in the spectrum of β-CaB$_4$O$_7$ are attributable to the higher resolution in the measurements. The large deviation of the first vibrational band at 1350 cm^{-1} from the value of 1450 cm^{-1} given for SrB$_4$O$_7$ results from the selection of the maximum of the very broad absorptions. The overall ranges of these broad absorptions are nearly identical in both spectra (β-CaB$_4$O$_7$: 1550–1300 cm^{-1}; SrB$_4$O$_7$: 1550–1350 cm^{-1}). The absorption peaks between 1100 and 800 cm^{-1} are those typical for the tetrahedral borate groups BO$_4$ as in YBO$_3$, GdBO$_3$, or TaBO$_4$ [65–67]. Between 1450 and 1100 cm^{-1} and below 800 cm^{-1} strong absorptions are observed, which are normally typical for triangular BO$_3$-groups as in LaBO$_3$ or EuB$_2$O$_4$ [70]. Since BO$_3$-groups are absent in β-CaB$_4$O$_7$ and SrB$_4$O$_7$, these absorptions have to be assigned to the corresponding OB$_3$-vibrations. The analogous geometry and similar force constants of the OB$_3$-group support this assignment, which is also con-
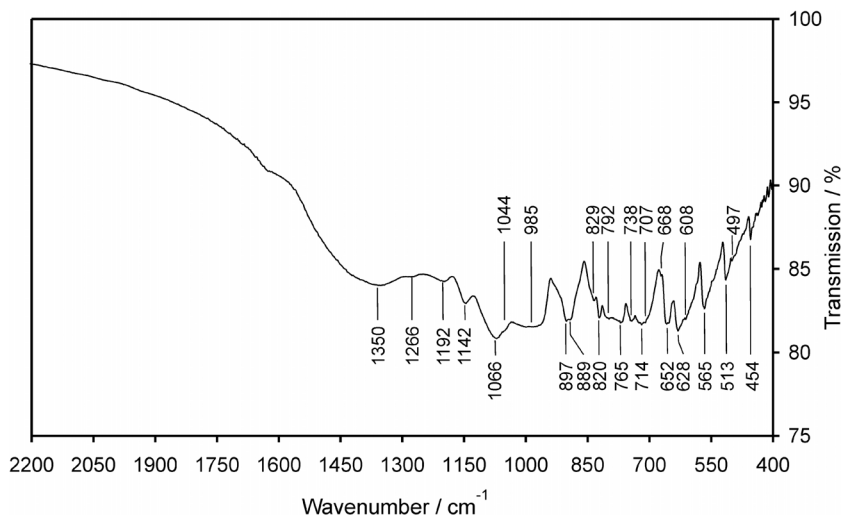
Fig. 6. Infrared spectrum of β-CaB$_4$O$_7$.

Tab. 8. Observed vibrational spectral data /cm^{-1} of β-CaB$_4$O$_7$ in comparison to SrB$_4$O$_7$ [64].

β-CaB$_4$O$_7$	SrB$_4$O$_7$ [64]
1350vbr	1450vbr
1266sbr	1256sbr
1192sbr	1232sbr
1142s	1166sbr
1066sbr	1045sbr
1044sh	1025sbr
985sbr	967sbr
897s	910mbr
889s	885s
829sh	
820s	808s
792sbr	
765sbr	765sbr
738s	722m
714sbr	703m
707sh	
668sh	
652s	657s
628s	639s
	622s
608sh	598msh
565s	551s
513s	510w
497sh	
454m	

Abbreviations. s: strong; sbr: strong broad; vbr: very broad; m: medium; sh: shoulder; w: weak.

firmed by IR-data of high-pressure boron oxide B$_2$O$_3$-II and of β-ZnB$_4$O$_7$ which also exhibit OB$_3$-groups next to BO$_4$-groups [46] and absorptions between 1550 and 1350 cm^{-1}. The existence of two crystallographically independent BO$_4$-units in the network structure of β-CaB$_4$O$_7$ in combination with OB$_3$-groups render a more detailed assignment of the vibrations difficult.

Conclusion

In this paper we described the multianvil synthesis of the new oxoborate β-CaB$_4$O$_7$ under a pressure of 7.7 GPa and at a temperature of 1100 °C. The structure was solved from single crystal data. Following the Pressure-Coordination rule [26] the coordination numbers of boron, calcium, and part of the oxygen atoms are increased in comparison to the α-modification. Specifically all boron atoms are four-coordinated, and the calcium atoms have coordination number 15 (in contrast to seven and eight in α-CaB$_4$O$_7$). For one quarter of the oxygen atoms in β-CaB$_4$O$_7$ the coordination is increased from two-fold to three-fold. As β-CaB$_4$O$_7$ is isotypic to the known phases SrB$_4$O$_7$, PbB$_4$O$_7$, and EuB$_4$O$_7$, it is also an illustrative example for the Pressure-Homologue rule. A comparison of the calculated densities of both modifications shows that the high-pressure modification β-CaB$_4$O$_7$ is much more dense (3.35 g/cm^3) than the normal-pressure modification α-CaB$_4$O$_7$ (2.69 g/cm^3).

[1] P. Becker, Adv. Mater. **10**, 979 (1998).

[2] T. Sasaki, Y. Mori, M. Yoshimura, Y. K. Yap, T. Kamimura, Mater. Sci. Eng. **30**, 1 (2000).

[3] D. A. Keszler, Curr. Opin. Solid State Mater. Sci. **1**, 204 (1996).

[4] H. Huppertz, B. von der Eltz, J. Am. Chem. Soc. **124**, 9376 (2002).

[5] H. Huppertz, Z. Naturforsch. **58b** (2003), in press.

[6] H. Emme, H. Huppertz, Z. Anorg. Allg. Chem. **628**, 2165 (2002).

[7] H. Emme, H. Huppertz, Chem. Eur. J. **9** (2003), in press.

[8] P. B. Hart, C. S. Brown, J. Inorg. Nucl. Chem. **24**, 1057 (1962).

[9] U. L. Schäfer, Neues Jahrb. Mineral., Monatsh. 75 (1968).

[10] Y. Ji, J. Liang, S. Xie, N. Zhu, Y. Li, Acta Crystallogr. **C49**, 78 (1993).

[11] N. V. Zayakina, A. A. Brovkin, Kristallografiya **21**, 502 (1976).

[12] U. L. Schäfer, Neues Jahrb. Mineral., Monatsh. 433 (1968).

[13] D. N. Shashkin, M. A. Simonov, N. V. Belov, Dokl. Akad. Nauk SSSR **195**, 345 (1970).

[14] D. P. Shashkin, M. A. Simonov, N. V. Belov, Sov. Phys. Crystallogr. **16**, 186 (1971).

[15] W. H. Zachariasen, Proc. Natl. Acad. Sci. U.S.A. **17**, 617 (1931).

[16] M. Marezio, H. A. Plettinger, W. H. Zachariasen, Acta Crystallogr. **16**, 390 (1963).

[17] M. Marezio, J. P. Remeika, P. D. Dernier, Acta Crystallogr. **B25**, 955 (1969).

[18] M. Marezio, J. P. Remeika, P. D. Dernier, Acta Crystallogr. **B25**, 965 (1969).

[19] A. Kirfel, Acta Crystallogr. **B43**, 333 (1987).

[20] W. Schuckmann, Neues Jahrb. Mineral., Monatsh. 142 (1969).

[21] J. Majling, V. Figusch, F. Hanic, V. Wiglasz, J. Corba, Mater. Res. Bull. **9**, 1379 (1974).

[22] A. Vegas, F. H. Cano, S. Garcia-Blanco, Acta Crystallogr. **B31**, 1416 (1975).

[23] I. Kusachi, C. Henmi, S. Kobayashi, Mineral. Mag. **59**, 549 (1995)

[24] B. Kindermann, Z. Kristallogr. **146**, 61 (1977).

[25] N. V. Zayakina, A. A. Brovkin, Sov. Phys. Crystallogr. **22**, 156 (1977).

[26] A. Neuhaus, Chimia **18**, 93 (1964).

[27] J. Krogh-Moe, Acta Chem. Scand. **18**, 2055 (1964).

[28] A. Perloff, S. Block, Acta Crystallogr. **20**, 274 (1966).

[29] F. Pan, G. Shen, R. Wang, X. Wang, D. Shen, J. Cryst. Growth **241**, 108 (2002).

[30] D. L. Corker, A. M. Glazer, Acta Crystallogr. **B52**, 260 (1996).

[31] K.-I. Machida, G.-Y. Adachi, J. Shiokawa, Acta Crystallogr. **B36**, 2008 (1980).

[32] H. Huppertz, Z. Naturforsch. **56b**, 697 (2001).

[33] D. Walker, M. A. Carpenter, C. M. Hitch, Am. Mineral. **75**, 1020 (1990).

[34] D. Walker, Am. Mineral. **76**, 1092 (1991).

[35] D. C. Rubie, Phase Trans. **68**, 431 (1999).

[36] P.-E. Werner, L. Eriksson, M. Westdahl, J. Appl. Crystallogr. **18**, 367 (1985).

[37] WinX$^{\text{POW}}$ Software, STOE & CIE GmbH, Darmstadt, (1998).

[38] A. L. Spek, PLATON – A Multipurpose Crystallographic Tool, Utrecht University, Utrecht, Netherlands (2002).

[39] G. M. Sheldrick, SHELXS-97, Program for the Solution of Crystal Structures, University of Göttingen, Germany (1997).

[40] G. M. Sheldrick, SHELXL-97, Program for Crystal Structure Refinement, University of Göttingen, Germany (1997).

[41] R. D. Shannon, C. T. Prewitt, Acta Crystallogr. **B25**, 925 (1969).

[42] J. R. Clark, Am. Mineral. **49**, 1549 (1964).

[43] J. A. Konnert, J. R. Clark, C. L. Christ, Am. Mineral. **55**, 1911 (1970).

[44] S. Ghose, C. Wan, Am. Mineral. **62**, 979 (1977).

[45] C. T. Prewitt, R. D. Shannon, Acta Crystallogr. **B24**, 869 (1968).

[46] H. Huppertz, G. Heymann, Solid State Sci., in press.

[47] W. E. Klee, Z. Kristallogr. **179**, 67 (1987).

[48] A. Beukemann, W. E. Klee, Z. Kristallogr. **209**, 709 (1994).

[49] A. Beukemann, W. E. Klee, Z. Kristallogr. **201**, 37 (1992).

[50] TOPOLAN – Topological Analysis of Crystal Structures, G. Thimm, S. Schumacher, W. Uhr, W. E. Klee, Universität Karlsruhe (1993).

[51] F. C. Hawthorne, P. C. Burns, J. D. Grice, in E. S. Grew and L. M. Anovitz (eds.): "Boron: Mineralogy, Petrology, and Geochemistry", Chap. 2, Reviews in Mineralogy 33, Mineralogical Society of America, Washington (1996).

[52] P. C. Burns, J. D. Grice, F. C. Hawthorne, Can. Mineral. **33**, 1131 (1995).

[53] J. D. Grice, P. C. Burns, F. C. Hawthorne, Can. Mineral. **37**, 731 (1999).

[54] J. A. Konnert, J. R. Clark, C. L. Christ, Z. Kristallogr. **132**, 241 (1970).

[55] J. D. Grice, R. A. Gault, J. van Velthuisen, Can. Mineral. **35**, 751 (1997).

[56] R. Hoppe, Angew. Chem. **78**, 52 (1966); Angew. Chem. Int. Ed. **5**, 95 (1966).

[57] R. Hoppe, Angew. Chem. **82**, 7 (1970); Angew. Chem. Int. Ed. **9**, 25 (1970).

[58] R. Hoppe, R. Hübenthal, MAPLE, Program for the Calculation of MAPLE- Values, Vers. 4, University of Gießen (1993).

[59] I. D. Brown, D. Altermatt, Acta Crystallogr. **B41**, 244 (1985).

[60] N. E. Brese, M. O'Keeffe, Acta Crystallogr. **B47**, 192 (1991).

[61] R. Hoppe, S. Voigt, H. Glaum, J. Kissel, H. P. Müller, K. Bernet, J. Less-Common Met. **156**, 105 (1989).

[62] S. Block, A. Perloff, Acta Crystallogr. **19**, 297 (1965).

[63] Yu. S. Oseledchik, A. L. Prosvirnin, A. I. Pisarevskiy, V. V. Starshenko, V. V. Osadchuk, S. P. Belokrys, N. V. Svitanko, A. S. Korol, S. A. Krikunov, A. F. Selevich, Opt. Mater. **4**, 669 (1995).

[64] C. E. Weir, R. A. Schroeder, J. Res. Nat. Bur. Stand. **86A**, 465 (1964).

[65] M. Ren, J. H. Lin, Y. Dong, L. Q. Yang, M. Z. Su, L. P. You, Chem. Mater. **11**, 1576 (1999).

[66] J. P. Laperches, P. Tarte, Spectrochim. Acta **22**, 1201 (1966).

[67] G. Blasse, G. P. M. van den Heuvel, Phys. Stat. Sol. **19**, 111 (1973).

[68] W. C. Steele, J. C. Decius, J. Chem. Phys. **25**, 1184 (1956).

[69] R. Böhlhoff, H. U. Bambauer, W. Hoffmann, Z. Kristallogr. **133**, 386 (1971).

[70] K. Machida, H. Hata, K. Okuno, G. Adachi, J. Shiokawa, J. Inorg. Nucl. Chem. **41**, 1425 (1979).